

## Chemical calcium phosphate precipitation using lime hydrates in a fluidized bed reactor

Leila Benmansour<sup>a,\*</sup>, Riad Eutamene<sup>a</sup>, Lakhdar Tifouti<sup>a</sup>, Khashayar Saleh<sup>b</sup>

<sup>a</sup>Laboratory of Environmental Engineering, Department of Process Engineering, Badji Mokhtar-Annaba University, P.O. Box: 12, 23000 Annaba, Algeria, Tel. +213 559 229 551; email: menadjliabenmansour1@yahoo.fr (L. Benmansour), Tel. +213 (0) 661 756 511; email: athameneriad@yahoo.fr (R. Eutamene), Tel. +213 (0) 38 87 10 57; email: ltifouti@yahoo.fr (L. Tifouti)

<sup>b</sup>EA TIMR 4297, Université de Technologie de Compiègne, Sorbonne Universités, 60200 Compiègne, France, Tel. +03 44 23 52 74; email: khashayar.saleh@utc.fr

Received 29 July 2020; Accepted 22 January 2021

### ABSTRACT

This study aimed to study the behaviour of the chemical precipitation of calcium phosphate by means of hydrated lime ( $\text{Ca}(\text{OH})_2$ ) using solutions with different concentrations of phosphate  $[\text{PO}_4^{3-}]$  ranging from 5 to 30 mg P/L. A hydrodynamic evaluation of the chemical precipitation of phosphates in a fluidized bed reactor (FBR) was carried out. Under optimal conditions relative to chemical precipitation of phosphates ( $\text{Ca}/\text{P} = 3$ ,  $\text{pH} = 9.6$ ,  $U_f = 0.58 \text{ cm s}^{-1}$  and  $T = 22^\circ\text{C}$ ), the phosphate removal efficiency  $\eta$  and the conversion  $\chi$  were 95% and 99%, respectively.  $[\text{PO}_4^{3-}]$  concentration in the outlet of FBR was lower than in pure water. A low and uncontrolled instantaneous elimination efficiency of 49%–71% was obtained. This work was also aimed at examining the effect of the porosity of the bed and the fluidization velocity, which are among the least impacting parameters, on the efficiency of the operation. The height of the fluidized bed is exceeded by 10%, with an expansion of  $H/H_{mf} = 2$ . There was a quasi-linear increase in expansion as a function of  $\text{PO}_4^{3-}$  concentration. The effect of  $\text{PO}_4^{3-}$  concentration on these different hydrodynamic parameters (i.e., expansion, porosity and fluidization velocity) was also investigated.

**Keywords:** Calcium phosphate; Chemical precipitation; Fluidized-bed reactor; Hydrodynamic behaviour; Phosphate concentration

### 1. Introduction

In the field of environmental prevention, several water treatment problems find solutions in the recovery and elimination of substances considered to be polluting at certain concentrations [1]. The large amount of phosphate present in wastewater is one of the main causes of eutrophication, which negatively affects many natural waterways. It is desirable that water treatment facilities remove phosphorus from wastewater before it is released into the environment [1]. Among these solutions, the recovery and

elimination of phosphates by the chemical precipitation process allow us to reuse these substances as raw material and prevent us from discharging into nature with uncontrolled doses. To maintain high P removal performance in the main stream, this phenomenon requires adequate treatment of the sludge or only the supernatants before their recirculation [1,2].

Regulations on the release of phosphate in several countries have been revised. For example, the release limit for total phosphorus in China has been reduced from 1.0 to 0.5 mg P/dm<sup>3</sup>[3].

\* Corresponding author.

Phosphate is a valuable, critical and non-renewable resource [4,5] and significantly contributes to agricultural and industrial development, for the production of fertilizers, food and pharmaceutical products [6–8].

Phosphate compounds found in wastewater or surface water have different origins: Runoff fertilizers, human and animal faeces, detergents and cleaning products. Total phosphate load includes ortho phosphates, polyphosphates, organic phosphorus compounds. Ortho- $\text{PO}_4$  is generally the most common compound. In water, phosphates come in dissolved, colloidal or solid form [9].

The chemical precipitation of calcium phosphates from wastewater and aqueous solutions has been the subject of much research, due to its importance in different fields such as industry, commerce, environment and health.

By recovering phosphate from wastewater, the effluent concentration decreases, eutrophication is reduced and the quality of the surrounding aquatic environment is improved. Therefore, recovery of phosphate as calcium phosphate can be seen as a promising method to achieve sustainable development [10].

Regarding the precipitate, Yigit and Mazlum [11] were interested in the nature of the precipitate and determined the optimal conditions for the removal of phosphate by carrying out a study first on real municipal wastewater, then on synthetic solutions. The results showed that struvite precipitation is more applicable for technical purposes while apatite precipitation is more applicable for economic reasons. Generally, some chemical compounds (iron salts, aluminum salts, lime milk) allow the precipitation of orthophosphate compounds in the form of metal phosphates with reduced solubility [9].

Few studies have appeared on the use of FBR for the elimination by adsorption of recalcitrant pollutants. Since the design and operation of FBR largely depend on experience and empirical approach, an understanding of important design and operating parameters is necessary for successful application of the technology [12]. Fluidized-bed reactor (FBR) occupies an important place in the process industry. It has been reported that RBFs have a number of advantages: the large solid–liquid interface surface area and the almost isothermal temperature distribution even for highly exothermic reactions, in addition, the pH and temperature control is easier [13].

In this work, the first screening study was done on the fluidized bed process with low inlet phosphate concentration ranging from 5 to 30 mg P/L.

On the other hand, parameters that may affect the removal efficiency of phosphate such as the mechanical stability of phosphate grain, the presence of impurities such as magnesium and carbonates was also investigated.

Although found in the environment, phosphorus occurs almost exclusively as phosphate, it exhibits complex speciation. It is either dissolved in water as an ionic compound resulting from the balance of forms of phosphoric acid according to pH ( $\text{H}_3\text{PO}_4$ ,  $\text{H}_2\text{PO}_4^-$ ,  $\text{HPO}_4^{2-}$  and  $\text{PO}_4^{3-}$ ), or participates in many organic compounds (oses, esters...) and inorganic distributed in solid and watery phases or in biological organisms [14]. The phosphorus associated with the solid phase exists in a wide variety of chemical forms, all of which constitute the “P-particulate”. Phosphate ions in

solution are main form of phosphorus directly assimilated by plants. The other forms are not, however, completely biologically inactive [14].

Wastewater phosphorus, particulate or soluble, is essentially made up of the following:

- Inorganic phosphorus (mainly polyphosphates) and orthophosphates, some of which comes from the hydrolysis of the former;
- Organic phosphorus: phospho-lipids, esters, polynucleotides, ATP, ADP.

Sodium and potassium phosphates are water soluble, monocalcic phosphates and magnesium phosphates are also soluble, but to a lesser extent. The other phosphates are insoluble. Total phosphorus is the sum of inorganic and organic phosphorus [15]. It has been established that orthophosphate is the preferred substrate for most microorganisms in the marine environment [16].

The World Health Organization (WHO) stipulates that the maximum concentration of phosphorus in discharged wastewater should be less than 0.5 mg/L [17]. The minimum requirements for wastewater treatment plants in Germany have significantly increased by phosphate regulations since 1989. The current limits of 2 mg/P<sub>total</sub> above a population of 20,000 and 1 mg/L P<sub>total</sub> above a population of 100,000 are likely to be even lower due to the harmonization of European standards. The total 2 mg/L limit of P will then apply to more than 10,000 in areas deemed sensitive by CE guidelines.

Improved elimination, adsorption and precipitation of biological phosphorus are well-established methods for the elimination of P. In most cases, P is removed from wastewater by forming insoluble or less soluble phosphate minerals. Among these minerals, calcium phosphate stands out because calcium phosphate precipitation can be obtained without dosing external calcium ions, as most natural and artificial aquatic systems have a favourable stoichiometric ratio for calcium phosphate formation. In addition, calcium phosphate is a preferred raw material for the fertilizer industry [18].

The process is based on the precipitation of calcium phosphate obtained by mixing a phosphate solution with calcium ions and a base. The base allows to move to the right of the chemical equilibrium given by Eq. (1), thus increasing the supersaturation [19]:



Therefore,  $\text{Ca}(\text{OH})_2$  in the solution may undergo the following chemical reaction:



Calcium and phosphate can be precipitated in different forms:  $\text{Ca}(\text{H}_2\text{PO}_4)_2$  (dicalcium dihydrogen phosphate),  $\text{Ca}(\text{H}_2\text{PO}_4)_2 \cdot 2\text{H}_2\text{O}$  (dicalcium phosphate dihydrate),  $\text{CaHPO}_4$  (calcium hydrogen phosphate),  $\text{CaHPO}_4 \cdot 2\text{H}_2\text{O}$  (calcium hydrogen phosphate dihydrate) and  $\text{Ca}_5(\text{PO}_4)_3(\text{OH})$

(hydroxyapatite). The apatite precipitation usually occurs within the pH range of 8–9.8 [11].

Chemical precipitation is a physico-chemical process, comprising the addition of a divalent or trivalent metal salt to wastewater, causing precipitation of an insoluble metal phosphate that is settled out by sedimentation. The most stable calcium phosphate compound is hydroxyapatite (PAH), the saturation concentration of which is not very high [6,11].

It was reported that lime is the most common calcium salt used for calcium phosphate precipitation, to provide simultaneous increases in both calcium and hydroxyl ions [20]. Seckler et al. [19] used the  $\text{Ca}(\text{OH})_2$  to recover phosphates from water model containing phosphate in concentration range between 5 and 100 mg P/L, with continuous-flow FBR. He found that the efficiency of 56% was achieved. He concluded that the nature of the solution used is the most influencing factor.

It should be noted that TCPA is in two crystalline forms:  $\alpha$ TCP and  $\beta$ TCP.

## 2. Materials and methods

Solution of phosphate was prepared using  $\text{Na}_2\text{HPO}_4 \cdot \text{H}_2\text{O}$  as a phosphate source of 1,000 mg  $\text{PO}_4^{3-}/\text{L}$  of distilled water, and left in a thermostatically controlled room (22°C).  $\text{Ca}(\text{OH})_2$  is used in the form of a 1,000 mg/L stock solution; maximum impurities:  $\text{Al}_2\text{O}_3$ : 0.17%,  $\text{Fe}_2\text{O}_3$ : 0.21%,  $\text{MgO}$ : 0.9%,  $\text{SiO}_2$ : 0.8%, S: 0.035%. The pH was adjusted by using NaOH with sodium bicarbonate as buffer solution to have a pH of 9.6.

The phosphate solutions used are synthesized with total content of 5–30 mg P/L of city water (the concentration of  $\text{PO}_4^{3-}$  is always expressed as the phosphorus content of

phosphates, 1 mg  $\text{P-PO}_4^{3-}/\text{L}$  corresponds to 3.07 mg  $\text{PO}_4^{3-}/\text{L}$ ). The physicochemical parameters of water are listed in Table 1.

A continuous fluidized bed reactor (36 L/h) with 5 cm in diameter and a total height column of 145 cm was used to investigate the precipitation of phosphate (Fig. 1). The column is filled with 0.4 kg of sand particles as a carrier of precipitating substances (CV32, SIBELCO – France), to obtain an expansion of 16 cm. The mean diameter of the quartz sand particles used was 226  $\mu\text{m}$  (denoted: Si-226). The average density was 2.6 and the shape factor was equal to 0.9. The porosity and velocity at the minimum of fluidization of sand are 0.56 and 0.1 cm/s, respectively. All experiments were conducted at room temperature 22°C and each one was repeated twice.

The first pump P-1 (Fig. 1) of the pre-prepared phosphate solution is first started with a low fluidization velocity

Table 1  
Physicochemical characteristics of water used

Parameters	Values
pH	7.4
$[\text{PO}_4^{3-}]$	2.46 (mg $\text{P-PO}_4^{3-}/\text{L}$ )
$[\text{Mg}^{2+}]$	21 (mg/L)
$[\text{Ca}^{2+}]$	106 (mg/L)
$[\text{Cl}^-]$	0.36 (mg/L)
$[\text{NH}_4^+]$	<0.05 (mg/L)
$[\text{NO}_3^-]$	25.1 (mg/L)
Conductivity at 20°C	710 ( $\mu\text{s cm}^{-1}$ )
Conductivity at 25°C	790 ( $\mu\text{s cm}^{-1}$ )

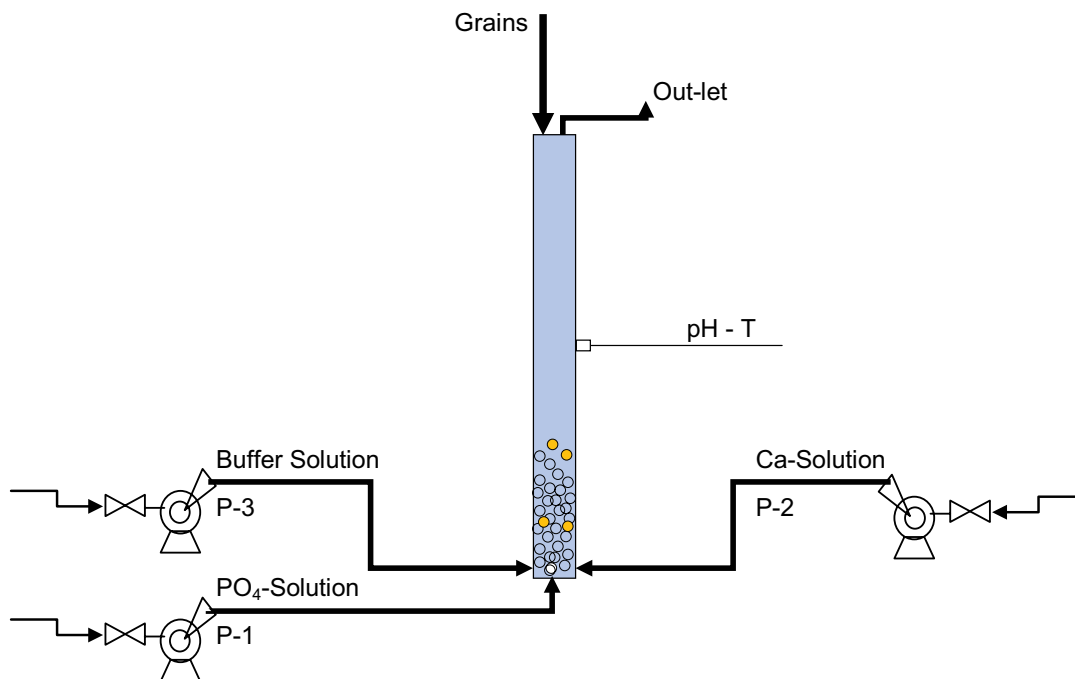


Fig. 1. Schema of the fluidized bed reactor.

(<math>U\_{mf}</math>) to prevent the escape of the carrier particles from the distributor, the carrier particles have then added by the upper part of the fluidized bed by means of a funnel.

The fluid flow rate is increased to an average value equivalent to  $U_{mf}$ . The pH of the solution was monitored at  $\pm 0.1$  unit throughout the experiment by P-3 (Fig. 1) injection of a buffer solution. The speed of injections was then raised to  $7U_{mf}$ . After the stabilization of pH solution, the  $\text{Ca}(\text{OH})_2$  solution was added continuously using a P-2 pump (Fig. 1). Finally, the process of the precipitation started. The duration of an experiment was fixed at 4 h.

Phosphate concentration was measured according to an ascorbic acid colorimetric method by PerkinElmer (Germany) Lambda 25 spectrophotometer at 882 nm wave length (APHA, 1985). In our phosphate precipitation experiments, the pH value is monitored by means of a universal sensor with an ALMEMO 2590-3S. The sand after each experiment is removed from the reactor, dried at  $600^\circ\text{C}$  for 12 h and analyzed by scanning electron microscopy (SEM, FEI HP 3600) and by a X-ray diffraction (XRD) to determine possible Ca-phosphate compounds on the surface of individual particles of the carrier material. The particle size distribution was determined by a Master sizer 2000 laser particle size analyzer from Malvern Instruments (UK).

*Data analysis:* The efficiency of phosphate removal and the conversion are given by the following equations [2,10]:

$$\eta = \frac{100 \cdot \left( [\text{PO}_4^{3-}]_{p,in} - [\text{PO}_4^{3-}]_{p,out} \right)}{[\text{PO}_4^{3-}]_{p,in}} \quad (3)$$

$$\chi = \frac{100 \cdot \left( [\text{PO}_4^{3-}]_{p,in} - [\text{PO}_4^{3-}]_{p,sol} \right)}{[\text{PO}_4^{3-}]_{p,in}} \quad (4)$$

where  $[\text{PO}_4^{3-}]_{in}$  denotes the initial phosphate concentration at the reactor inlet, mg P/L;  $[\text{PO}_4^{3-}]_{out}$  denotes the total phosphate concentration in the dissolved form in the reactor (without filtration), mg P/L;  $[\text{PO}_4^{3-}]_{sol}$  denotes the solute phosphate concentration (with filtration at the reactor outlet), mg P/L.

These parameters are also good indicators of the phosphate removal and provide important information on the precipitation process. The difference between the efficiency of the precipitation and the efficiency of the recovery is due to the fine crystals loss in the reactor. On the other hand, the behaviour of the chemical precipitation by a hydrodynamic evaluation has not been investigated.

The expansion of the fluidized bed is defined experimentally as the fraction between the average porosity and the porosity at the minimum fluidization velocity. It is determined by the following expression:

$$\frac{H}{H_{mf}} = \frac{(1 - \epsilon_{mf})}{(1 - \epsilon)} \quad (5)$$

Porosity is defined by:

$$\epsilon = \frac{(V_{Exp} - V_{sp}M)}{V_{Exp}} \quad (6)$$

in which  $M$  is the mass of particles within the reactor,  $V_{Exp}$  is the total volume and  $V_{sp}$  is the specific volume of particles. The fluidization velocity of particles is determined as:

$$U_f = \frac{w}{S} \quad (7)$$

The specific surface area can be calculated using the following equation [12]:

$$a_s = \frac{6(1 - \epsilon)}{d \times \psi} \quad (8)$$

where  $a_s$ : specific surface area ( $\text{m}^{-1}$ );  $\epsilon$ : bed porosity;  $d$ : support particle diameter (mm);  $\psi$ : shape factor (dimensionless);  $w$ : fluid (volume) flow rate ( $\text{m}^3\text{s}^{-1}$ ).

### 3. Results and discussion

The minimum and maximum of phosphate removal efficiency obtained in this series was 28% and 91%, respectively. The influence of phosphate concentration on the various parameters is presented below.

#### 3.1. Effect of $\text{PO}_4^{3-}$ concentration in the phosphate removal efficiency

This section mainly focuses on the influence of the initial concentration of the phosphate feed solution on the final qualities and quantities of the calcium phosphate particles and on the various hydrodynamic parameters. The phosphate concentration was changed from 5 to 30 mg P/L and the molar ratio was set at a Ca/P = 3. It is very important to point out that these operating conditions are not arbitrary conditions. A preliminary study was carried out in order to determine the optimum of the inlet molar ratio Ca/P used in this study. Ca/P equal 3 was used, with an average and acceptable phosphate removal efficiency of 80% for a phosphate concentration of 10 mg P/L. This allowed to have the effectiveness of different phosphate concentrations from 80% to 100%.

Fig. 2 shows phosphate removal efficiency during the precipitation test as a function of the fluidization time  $t_f$ .  $\text{PO}_4^{3-}$  concentration used is 5, 10, 20 and 30 mg P/L. The phosphate removal efficiency increased from 50% to 81%, 91% and 86%, respectively. When the  $\text{PO}_4^{3-}$  concentration in the mixture reached 20 and 30 mg P/L, feed solutions were transformed to pure water.

It should be noted, however, that the removal efficiency of phosphate using  $\text{PO}_4^{3-}$  concentration of 20 mg P/L is relatively high compared with those found in other experiments. We also note that, for the concentrations: 10, 20 and 30 mg P/L, the same change trend is observed as a function of the time (Fig. 2a), with a greater efficiency for the second configuration (20 mg P/L), with a removal efficiency and a fluidization of the order of 91% and 0.98, respectively. From 20 mg P/L, the amount of phosphorus rejected is less than 2 mg P/L and the precipitate is completely removed in the fluidized bed. These results indicate that the hydrated lime can be applied for the precipitation of phosphate with comparable success, providing further

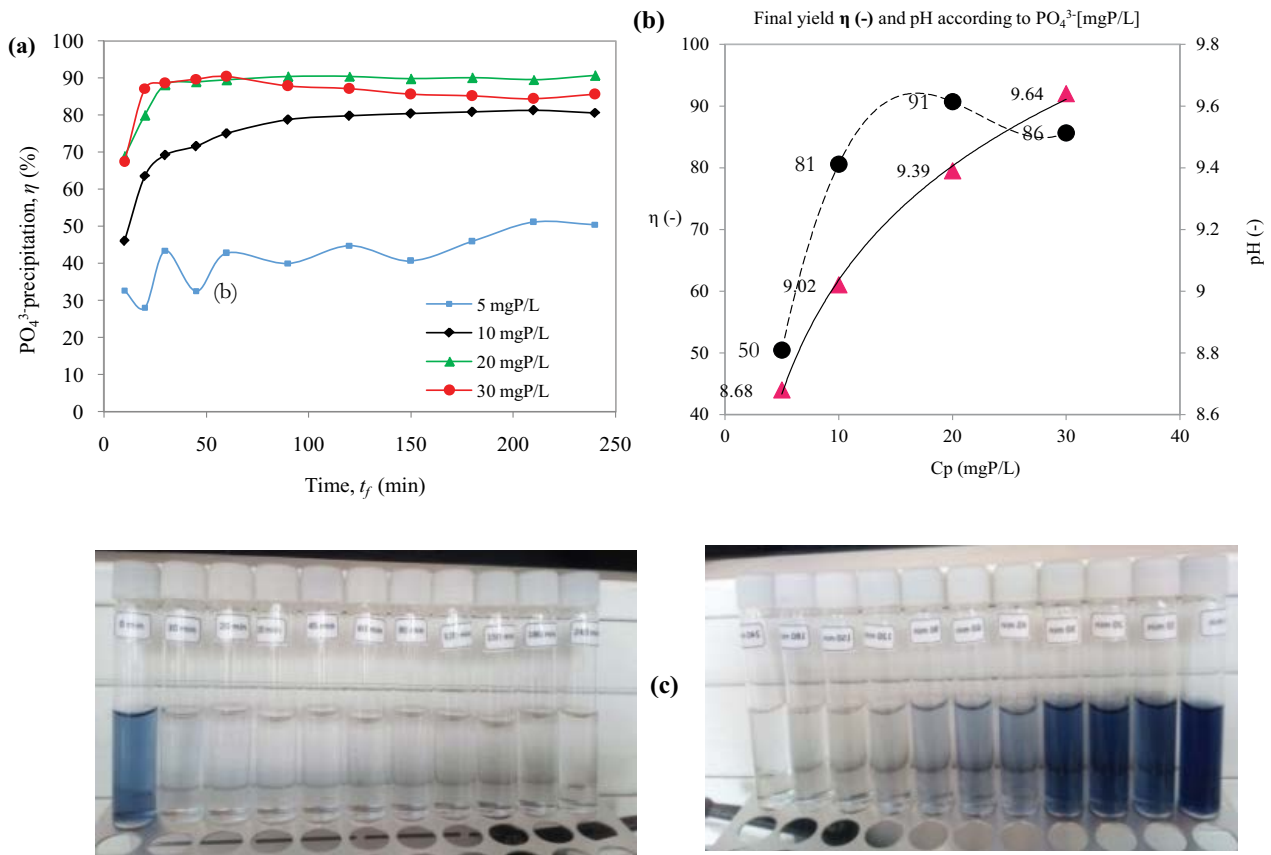


Fig. 2. Phosphate removal efficiency in the samples fluidized for 4 h, as a function of: (a) the precipitation time, (b) PO<sub>4</sub><sup>3-</sup> concentration, using sand as seed and water spiked with 5–30 mg P/L (c) (T = 22°C, Ca/P = 3, Si-226).

simplification for phosphate removal. PO<sub>4</sub><sup>3-</sup> concentration obtained is better than that previously reported by Seckler et al. [19]. This difference can be attributed to the operation conditions employed. The Ca ions in this study may play dual function to raise the solution pH from 8.5 to 9.6, and to provide the calcium phosphate precipitation in the mixture.

Fig. 2b clearly reflects the reduction in the phosphate removal efficiency for a concentration of 30 mg P/L after 60 min. Under these operating conditions, our results are in agreement with those of Yigit and Mazlum [11] as can be seen from the analysis results depicted in Fig. 2.

Thus, the high Ca and PO<sub>4</sub><sup>3-</sup> concentrations significantly affect the quality of chemical precipitation of phosphates. This effect is shown in Fig. 2. The reduction in the precipitation efficiency is caused by the high pH values. Particularly, the presence of carbonate ions holds up the precipitation process [11]. Additionally, the presence of fluoride and magnesium ions influences the type and shape of calcium phosphate. Since efficiency and conversion are related, the same observations and trends were observed with the conversion of precipitation.

Influence of an increasing concentration on the conversion is shown in Fig. 3. In the presence of 30 mg P/L, the conversion is decreased by 0.73%. The precipitation of calcium phosphate strongly depends on the pH of the solution and the concentration of the mixing solutions [11,10].

The following points can explain the growth of the residual phosphate concentration in the FBR as a function of the initial phosphate concentration:

- [PO<sub>4</sub><sup>3-</sup>] = 5 mg P/L                      pH = 8.68

For low concentrations of Ca(OH)<sub>2</sub> and PO<sub>4</sub><sup>3-</sup>, a low pH is obtained, which generally leads to the precipitation of a small amount, in the first hand, of amorphous calcium phosphate at low pH values (to 8.5).

- [PO<sub>4</sub><sup>3-</sup>] = 10 and 20 mg P/L              pH = 9.02 and 9.39

These conditions generally result in the formation of amorphous calcium phosphate ACP (Ca<sub>3</sub>(PO<sub>4</sub>)<sub>2</sub>) at an optimum Ca/P-1.5 or hydroxyapatite HAP Ca<sub>5</sub>(PO<sub>4</sub>)<sub>3</sub>OH at an optimum Ca/P-1.33 or Ca/P-1.67.

- [PO<sub>4</sub><sup>3-</sup>] = 30 mg P/L                      pH = 9.64

For a pH above 9.5, the conditions are favourable for the precipitation of the HAP with a high excess of calcium, which favors the precipitation. This explains the increase in precipitation of phosphates in an FBR. In these conditions, there is a decrease in the phosphate removal efficiency. This may be due to the low concentrations of impurities of magnesium Mg and carbonate CO<sub>3</sub> in the bed [19,7].

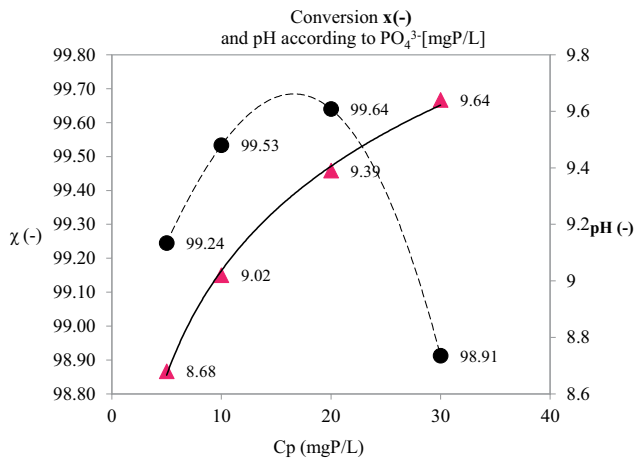


Fig. 3. Change of the conversion as a function of  $\text{PO}_4^{3-}$  concentration, using sand as seeds and water spiked with 5–30 mg P/L ( $T = 22^\circ\text{C}$ ,  $\text{Ca/P} = 3$ ,  $\text{Si-226}$ ,  $U = 0.58 \text{ cm/s}$  and  $t_f = 4 \text{ h}$ ).

Furthermore, in order to prevent fine particles formation and increase the efficiency of the process, the phosphate concentration at the bottom of the reactor has to be kept below a critical value [ $\text{PO}_4^{3-} = 30 \text{ mg P/L}$ ]. The precipitation of calcium and phosphate should be present in the medium at a minimum concentration.

### 3.2. Effects of $\text{PO}_4^{3-}$ concentration on different hydrodynamic parameters

In this order, all of the hydrodynamic parameters such as the bed expansion, the bed porosity and thus the fluidization velocity were determined. This is the first study reporting the effect of calcium phosphate precipitation on hydrodynamic parameters. Fig. 4 shows the expansion profiles as a function of  $\text{PO}_4^{3-}$  concentration in the fluidized bed with  $\text{Ca/P} = 3$ . It follows the same evolution of the expansion as a function of time. From the first minute, the bed starts to expand. The increase in the  $\text{PO}_4^{3-}$  in the mixture was increased by an increase in the expansion of the fluidized bed. Expansion increased from 1.5 to 2.7 after 4 h.

For [ $\text{PO}_4^{3-} = 5$  and  $10 \text{ mg P/L}$ ]: for the first part (Fig. 4), the expansion increased with an increase in the fluidization time, there is a slight increase in the two configurations. When the fluidization time increased from 1 to 60 min, the expansion increased from 1.46 to 1.48 and from 1.58 to 1.67, respectively. For the second part (Fig. 4), the expansion is gradually plateaued between 90 and 240 min. [ $\text{PO}_4^{3-} = 5 \text{ mg P/L}$  is classified as a concentration that reacts poorly with phosphate  $\eta = 41\%$ .

For [ $\text{PO}_4^{3-} = 20$  and  $30 \text{ mg P/L}$ ]: as seen in Fig. 4, we notice a high expansion. The expansion is carried out with a rapid tendency during the first minute of the experiment from 1.63 to 2.2 and 1.66 to 2.66, respectively. The expansion of the bed is an important component for the understanding of the calcium phosphate removal. The maximum expansion corresponding to the maximum efficiency. At a temperature of  $22^\circ\text{C}$ , our experiments confirm the influence of  $\text{PO}_4^{3-}$  concentration on the expansion of the bed. From  $10 \text{ mg P/L}$  and  $\text{Ca/P} = 3$ , the amount of phosphate rejected is less than

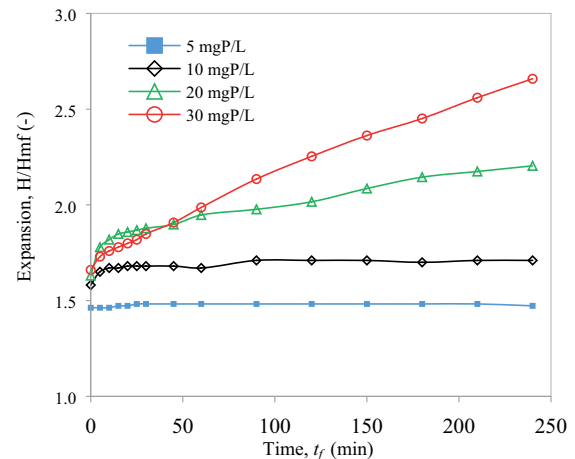


Fig. 4. Evolution of the expansion as a function of the time, using sand as seed and water spiked with 5–30 mg P/L.

$2.1 \text{ mg P/L}$  and the precipitate is completely retained in the fluidized bed.

Fig. 5 shows the fluidization velocity during the precipitation tests as a function of the fluidization time  $t_f$ . The fluidization velocity is  $0.574 \text{ cm/s}$ . It was increased after 4 h: for the concentrations 5 and  $10 \text{ mg P/L}$  and is, respectively, for the concentrations 20 and  $30 \text{ mg P/L}$   $0.579$  and  $0.581$ .

The height of the fluidized bed is exceeded by 10% of the bed, with an expansion of  $H/H_{mf} = 2$ . There is a quasi-linear increase in expansion as a function of  $\text{PO}_4^{3-}$  concentration. Although the efficiency is limited by a  $\text{PO}_4^{3-}$  concentration value of  $20 \text{ mg P/L}$ , a quasi-linear increase in the bed height as a function of time is always observed and this parameter is not related to the efficiency of precipitation. There is only one reason for this: for a  $\text{PO}_4^{3-}$  concentration of  $30 \text{ mg P/L}$  there is a large formation of the fine particles, which escape from the column, which otherwise represents a slight decrease in the efficiency and of the conversion of the fluidized bed. Thus, it can be concluded that a  $\text{PO}_4^{3-}$  concentration of  $20 \text{ mg P/L}$  is the limit of precipitation in our case.

Fig. 5 shows the evolution of the  $U_f$  as a function of time for a velocity of the liquid varied from  $0.559$  to  $0.581 \text{ cm s}^{-1}$ , it is clearly seen that there is always an increase in the fluidization velocity as a function of the  $\text{PO}_4^{3-}$  concentration for the four configurations studied, indicating that the average diameter of the particles is slightly increased.

The final porosity is  $0.639$  for  $10$  and  $20 \text{ mg P/L}$  then increases to  $0.644$  with an increase in the concentration of  $\text{PO}_4^{3-}$  ( $30 \text{ mg P/L}$ ). These variations in the porosity curves can be attributed to the change in the structure of the bed due to the entrainment to the surface of the bed of the fine particles trapped by the large particles. These variations disappear at  $\text{PO}_4^{3-}$  concentration lower than  $20 \text{ mg P/L}$  of the mixture corresponding to an average particle diameter of less than  $295 \mu\text{m}$ .

### 3.3. Properties of the solids

Sand morphology before and after precipitation of phosphate was examined by scanning electron microscopy.

SEM images show an increase in the average diameter  $d_p$  of the particles during the manipulation, which confirms a good coating (Fig. 6). From the particles size distribution of the sand particles shown in Fig. 7 before and after precipitation, it is clearly seen that the  $d_p$  of particles is significantly increased from 226 to 300  $\mu\text{m}$ .

These distributions clearly confirm that there is an increase in the average particle diameter for the four studied configurations 5, 10, 20 and 30 mg P/L corresponding

to a final average particle diameter  $d_p$  of 271, 274, 295 and 300  $\mu\text{m}$ , with an increase of 19.9%; 21%; 30.7% and 32.7%, respectively. On the other hand, the specific surface area of the particles after precipitation is increased by 184  $\text{cm}^2/\text{g}$  for Si-226 to 228; 226; 209 and 207  $\text{cm}^2/\text{g}$  for the different studied concentrations of 5 to 30 mg P/L respectively.

X-ray diffraction determines the nature of the crystalline phases. Precipitates formed at pH 9.4 with a molar

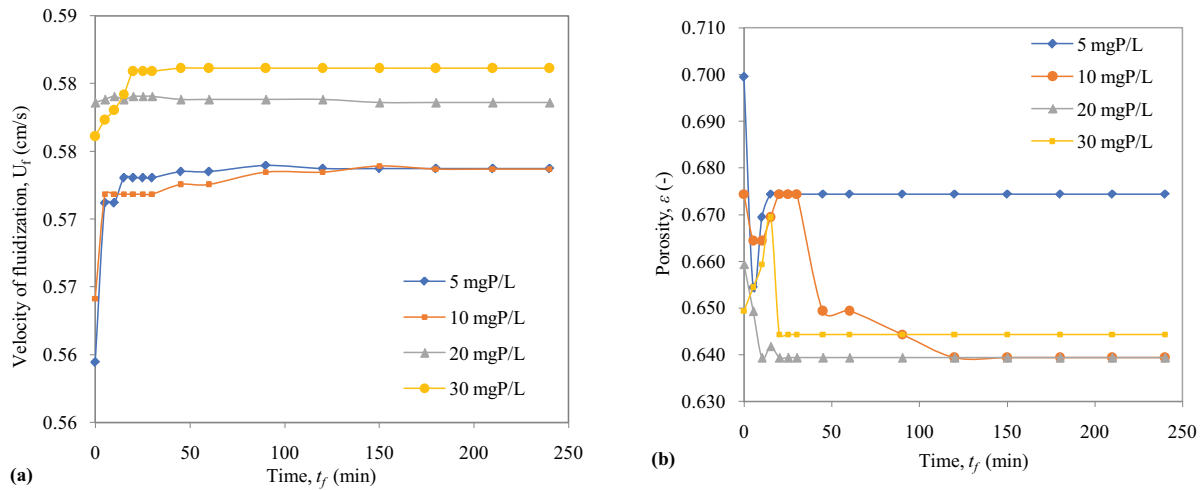


Fig. 5. Evolution of the velocity of fluidization (a) and the porosity of the bed (b) as a function of the time, using sand as seed and water spiked with 5–30 mg P/L.

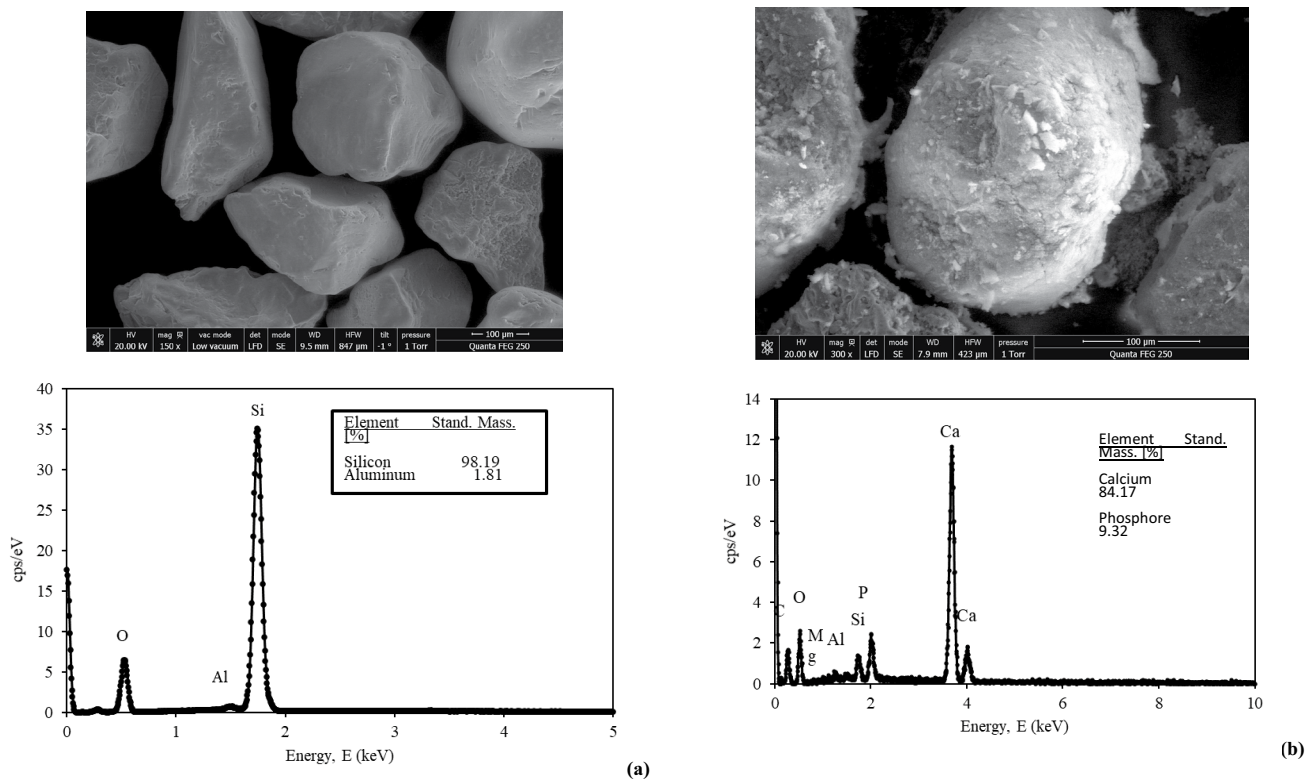


Fig. 6. SEM images of sand particles (a) before and (b) after precipitation (20 mg P/L).

ratio (Ca/P = 3) were analyzed by XRD in Fig. 8. A few characteristic peaks of  $\beta$ TCP were found in the precipitate.

Also from the presentation of the results obtained by the morphology G3, and the analysis of 2D images of a particle in 3D and calculation of various parameters of size and shape, namely: the equivalent volume of sphere  $V_{ES}$  (i.e., the volume of a sphere of the same volume of a particle in 3D), the circularity and the solidity of the particles, the various previous parameters determined for the four studied configurations 5, 10, 20 and 30 mg P/L are grouped together in Table 2.

It is generally stated that for phosphate concentration values of 5 and 10 mg P/L, precipitation is poor, and for values of 20 and 30 mg P/L, precipitation is moderately easy and effective.

From the results of Table 2, we can propose a classification of the efficiency of the phosphate precipitation by lime of the following tested concentrations:

- The equivalent volume parameter: 30 mg P/L > 20 mg P/L > 5 mg P/L > 10 mg P/L.
- The solidity parameter: 20 mg P/L > 30 mg P/L > 10 mg P/L > 5 mg P/L.
- The circularity parameter: 10 mg P/L > 5 mg P/L > 20 mg P/L > 30 mg P/L.

The classification of the precipitation of calcium phosphates according to the parameter of the initial

phosphate concentration is proportional to the initial phosphate concentrations at the inlet of the fluidization column.

#### 4. Conclusions

This work assessed the FBR process for the treatment of synthetic water containing calcium and phosphate. The process of removing phosphates by precipitation for concentrations ranging from 5 to 30 mg P/L reaches a maximum value for 20 mg P/L. The  $PO_4^{3-}$  concentration significantly affects the fluidization rate and the

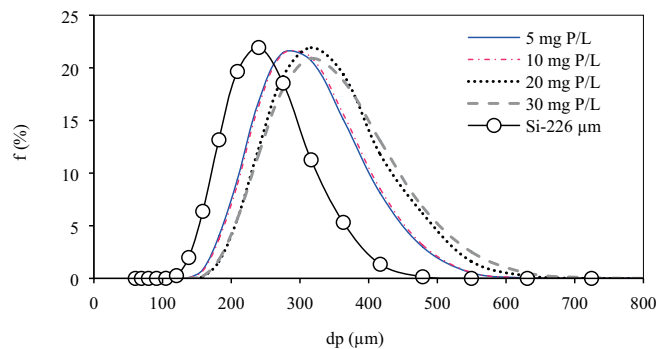


Fig. 7. Particle size distribution of sand particles before and after precipitation for different concentrations.

Table 2  
Different parameters determined by the morphology photo

[PO <sub>4</sub> ] mgP/L	V <sub>ES</sub> (μm <sup>3</sup> )	Solidity (-)	Circularity (-)	HS Circularity (-)	S <sub>sp</sub> (μm <sup>2</sup> )
5	15 × 10 <sup>6</sup>	0.972	0.910	0.863	66,000
10	14 × 10 <sup>6</sup>	0.972	0.923	0.862	64,000
20	16.6 × 10 <sup>6</sup>	0.973	0.925	0.859	81,000
30	17.5 × 10 <sup>6</sup>	0.975	0.924	0.854	78,000

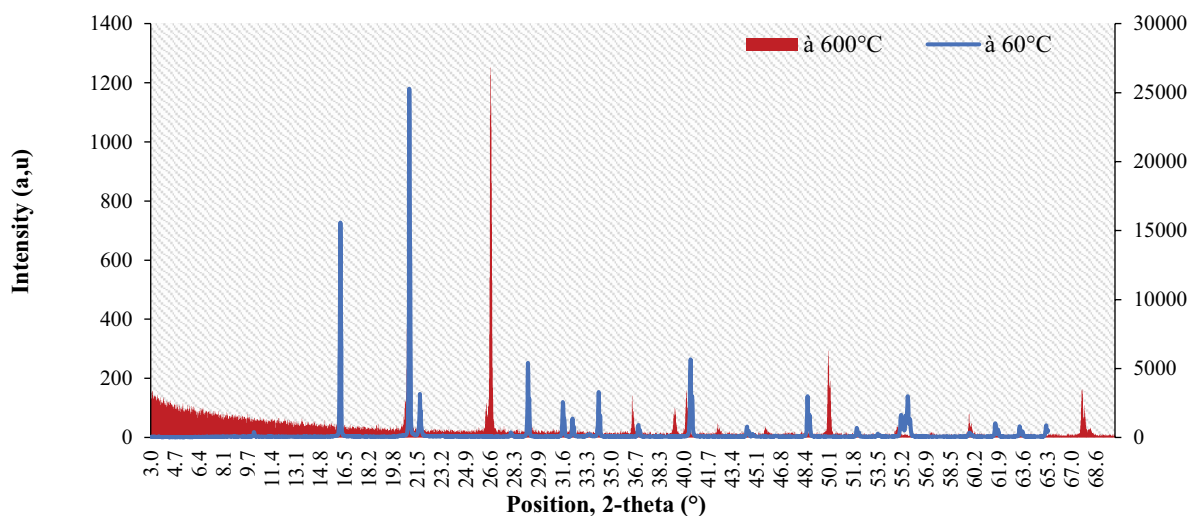


Fig. 8. X-ray diffractogram of coated sand particles at a concentration of 20 mg P/L.

porosity of the fluidized bed (the maximum expansion corresponding to the maximum efficiency). The particle size distributions for the four studied configurations: 5, 10, 20 and 30 mg P/L, clearly confirmed that there is an increase of the final average particle diameter  $d_p$  to 25%. The maximum expansion corresponding to the maximum efficiency. SEM and XRD analyses have shown that the precipitate has a chemical composition close to that of  $\beta$ TCP.

### Acknowledgement

The authors are grateful to the Chemical Engineering Department, University of Technology (UTC/TIMR EA 4297) of Compiegne, France, for providing instrumentation facilities. The authors would like to acknowledge Pr. André PAUSS (UTC/TIMR EA 4297) for his valuable help.

### References

- [1] L.E. de-Bashan, Y. Bashan, Recent advances in removing phosphorus from wastewater and its future use as fertilizer (1997–2003), *Water Res.*, 38 (2004) 4222–4246.
- [2] P. Battistoni, B. Paci, F. Fatone, P. Pavan, Phosphorus removal from supernatants at low concentration using packed and fluidized-bed reactors, *Ind. Eng. Chem. Res.*, 44 (2005) 6701–6707.
- [3] A. Sonoda, Y. Makita, Y. Sugiura, A. Ogata, C. Suh, J.H. Lee, K. Ooi, Influence of coexisting calcium ions during on-column phosphate adsorption and desorption with granular ferric oxide, *Sep. Purif. Technol.*, 249 (2020) 117143.
- [4] D. Cordell, J.O. Drangert, S. White, The Story of Phosphorus: Global Food Security and Food for Thought, *Global Environ. Change*, 19 (2009) 292–305.
- [5] U. Berg, D. Donnert, A. Ehbrecht, W. Bumiller, I. Kusche, P.G. Weidler, R. Nüesch, Active filtration for the elimination and recovery of phosphorus from waste water, *Colloid Surf., A*, 265 (2005) 141–148.
- [6] G.K. Morse, S.W. Brett, J.A. Guy, J.N. Lester, Review: phosphorus removal and recovery technologies, *Sci. Total Environ.*, 212 (1998) 69–81.
- [7] F. Abbona, H.E. Lundager Madsen, R. Boistelle, The initial phases of calcium and magnesium phosphates precipitated from solutions of high to medium concentrations, *J. Cryst. Growth*, 74 (1986) 581–590.
- [8] Y. Satoshi, O. Seichiro, H. Hiroyuki, A. Kotaro, Y. Mitoma, K. Hidetaka, B. K. Biswas, Simultaneous crystallization of phosphate and potassium as magnesium potassium phosphate using bubble column reactor with draught tube, *J. Environ. Chem. Eng.*, 1 (2013) 1154–1158.
- [9] P. Pütz, Elimination and Determination of Phosphates, Practice Report, Laboratory Analysis and Process Analysis, Nutrients Phosphate, Hach Lange United for Water Quality, 2008, pp. 1–4.
- [10] A.T.K. Tran, Y. Zhang, D. De Corte, J.B. Hannes, W. Ye, P. Mondal, N. Jullok, B. Meesschaert, L. Pinoy, B.V.D. Bruggen, P-Recovery as calcium phosphate from wastewater using an integrated selectrodialysis/crystallization process, *J. Cleaner Prod.*, 77 (2014) 140–151.
- [11] N.Ö. Yigit, S. Mazlum, Phosphate recovery potential from wastewater by chemical precipitation at batch conditions, *Environ. Technol.*, 28 (2007) 83–93.
- [12] M.M. Bello, A.A. Abdul Raman, M. Purushothaman, Applications of fluidized bed reactors in wastewater treatment – a review of the major design and operational parameters, *J. Cleaner Prod.*, 141 (2017) 1492–1514.
- [13] F. Tisa, A.A. Abdraman, W.M.A. Wan daud, Applicability of fluidized-bed reactor in recalcitrant compound degradation through advanced oxidation processes: a review, *J. Environ. Manage.*, 146 (2014) 260–275.
- [14] C. Pistocchi, F. Tamburini, L. Savoye, M. Sebito, I. Baneschi, D. Lacroix, P. Perney, J.M. Dorioz, Développement d'une méthode d'extraction et purification des phosphates à partir de matrices sédimentaires pour l'analyse isotopique de leur oxygène, *Le Cahier des Techniques de l'INRA*, 81 (2014) 1–23.
- [15] D. Deronzier, J.M. Choubert, Traitement du phosphore dans les petites stations d'épuration à boues activées, Document Technique, FNDAE n° 29, Cemagref, 2004.
- [16] X. Zhu, J. Ma, Recent advances in the determination of phosphate in environmental water samples: insights from practical perspectives, *Trends Anal. Chem.*, 127 (2020) 115908.
- [17] Y. Zhao, L. Guo, W. Shen, Q. An, Z. Xiao, H. Wang, W. Cai, S. Zhai, Z. Li, Function integrated chitosan-based beads with throughout sorption sites and inherent diffusion network for efficient phosphate removal, *Carbohydr. Polym.*, 230 (2020) 115639.
- [18] Y. Lei, E. Geraets, M. Saakes, D. Renata, V. Weijden, Cees. J.N. Buisman, Electrochemical removal of phosphate in the presence of calcium at low current density: precipitation or adsorption, *Water Res.*, 169 (2020) 115207.
- [19] M.M. Seckler, O.S.L. Bruinsma, G.M. Van Rosmalen, Calcium phosphate precipitation in a fluidized-bed in relation to process conditions: a black box approach, *Water Res.*, 30 (1996) 1677–1685.
- [20] S. Yeoman, T. Stephenson, J.N. Lester, R. Perry, The removal of phosphorus during wastewater treatment: a review, *Environ. Pollut.*, 49 (1988) 183–233.